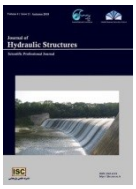
Journal of Hydraulic Structures
J. Hydraul. Struct., 2020; 6(3):59-82
DOI: 10.22055/jhs.2020.33293.1137



OPEN ACCESS

Shape Optimization of Concrete Arch Dams with SPSA Algorithm and Post-analysis of Pareto Front for selection the Best Alternatives

Majid Pouraminian[1]
Somayyeh Pourbakhshian [2]

Abstract

The optimization of structure shapes is a challenging endeavor in many fields of engineering since the generation of a parametrical model and numerical solutions of the model in the optimization process may have heavy computational costs. In the present study, a methodology is presented for the design of shape optimization of high arch dams to simultaneously reduce dam construction costs and increase the dam body safety by considering stage construction. Structural optimization is performed for permanents loads, including dam body weight and the hydrostatic pressure of the reservoir water. To simulate concreting, the dam body weight is considered through an eight-stage loading. The Simultaneous Perturbation Stochastic Approximation (SPSA) optimization algorithm is employed to find the optimized shape using the simple additive weighting method. The VIKOR method is used to decide upon the optimized shape of the dam. The proposed methodology greatly assists analysts with little experience in designing. It also helps decide upon the preferred solution from among optimal solutions.

Keywords: Double curvature concrete arch dam, Multi-objective Shape Optimization, Pareto Front, Decision Making, VIKOR, Sum weighted SPSA Algorithm.

Received: 17 April 2020; Accepted: 19 December 2020

1. Introduction

Dams are the infrastructural structures of all countries. So far, a relatively large number of studies have been conducted on the minimization of dam construction costs. This is because most concrete dam construction costs are spent on the concrete used in dam body [1]. Therefore,

[1] Department of Civil Engineering, Ramsar Branch, Islamic Azad University, Ramsar, Iran m.pouraminian@iauramsar.ac.ir; majid.pouraminian@gmail.com **(Corresponding author)**
[2] Department of Civil Engineering, Ramsar Branch, Islamic Azad University, Ramsar, Iran s.pourbakhshian@iauramsar.ac.ir.

by optimizing the volume of concrete, 5-20% of the concrete used in body dams can be saved. As the volume of concrete used in high arch dams adds up to millions of cubic meters, this ratio shows a considerable saving in concrete. Some studies [2-9] attempt to minimize dam construction costs by considering the volume of concrete. In these studies, the dam safety criterion, strength demand of the structure for bearing probable loads, and safety factors have been included in the constraints of the optimization problem. In optimization of engineering problems, the multi-objective optimization is more realistic than single-criterion optimization. Therefore, some other studies have tried to simultaneously minimize concrete and maximize the tensile stress of body dam as cost criterion and safety criterion, respectively. In these studies, the compressive strength demand and safety factor required for compressive stresses are included in the optimization problem as constraints [10-13]. For the first time, the bin-objective algorithm Sum-weighting SPSA (SW-SPSA) has been utilized in the multi-objective optimization of the shape of concrete arch dams. MATLAB was used to execute the optimization algorithm, and the batch mode of the finite-element software was employed to analyze the structure. To perform the optimization, an integrated program called MATLAB-APDL was written by the authors [14].

In bin-objective optimization problems, contrary to optimization using a single objective function, the solution of the problem is not merely a single optimal solution but a set of optimal solutions, that namely a set of non-dominated alternatives. Therefore, methods must be considered to help decision-makers in deciding upon the optimal shape from among optimal solutions. In some studies [14,15] by development and Investigating Pareto Front attempt to choose best alternatives. In the present study, the VIKOR method was used to select the preferred solution from the Pareto front [16].

2. Mathematical equation of arch dam design

2.1. Preliminary design

The vectors of geometrical variables required for defining the primary design of the dam include: t_C, t_{AL}, t_{AR}, Y_U, Y_D, R_{UL},R_{UR}, R_{DL}, R_{DR}, X_{eL} and X_{eR} respectively denote the thickness of the crown cantilever and the thickness of the left and right abutment, upstream and downstream profile of the crown cantilever, radius of the left and right curvature, upstream and downstream face, left and right abutment curve on the upstream face.

2.2. The geometrical model of the arch dam

For the optimized design of the shape of arch dams, the geometrical shape must be designed based on dam behavior.

2.2.1. Crown cantilever shape

In the present paper, to define the shape of the crown cantilever, two functions are used: an elliptic conic function for the upstream face, and a third-degree polynomial function for the thickness of the cantilever, based on Table 1. Parameters of a, b, c, d, e (value of f=-1) are determined using the variables in $Y_1, Y_6, Y_9, Y_{12}, Y_{16}$ in levels $Z_b(at.base), Z_{lb}(at.0.26H)$, $Z_{lu}(at.0.49H), Z_u(at.0.72H), Z_c(at.crest)$. Thus, using the equation $U_w(Z)$ and the determined coefficients, the projection of the upstream cantilever is obtained at any height. Then, the downstream projection at that height is obtained by summing

the upstream projection and the thickness of the crown cantilever.

2.2.2. Equation of thickness curve

The thickness of the crown cantilever and abutments at the selected height Z of the third-degree function is determined based on Table 1 as follows: Parameter a_0, a_1, a_2, a_3 are determined using the variables in $t_{C1}, t_{C7}, t_{C11}, t_{C16}$ at levels of $Z_b(at.base), Z_l(at.0.34H), Z_u(at.0.65H)$ and $Z_c(at.crest)$. Thus, using the equation $t_C(Z)$ and the determined coefficients, the thickness of the crown cantilever is obtained at any height. The left and right thickness of abutments is calculated using the same procedure.

2.2.3 The equation of radius of curvature

The equation of radius of curvature at the selected height Z of the third-degree function is determined based on Table 1 as follows: Parameters d_0, d_1, d_2, d_3 are determined using the variables in $R_{UL1}, R_{UL7}, R_{UL11}, and R_{UL16}$ at levels of $Z_b(at.base), Z_l(at.0.34H), Z_u(at.0.65H)$ and $Z_c(at.crest)$. Thus, using the equation $R_{UL}(Z)$ and the determined coefficients; the equation of radius of curvature is obtained at any height. Other arch radii are calculated using the same procedure.

2.2.4 The horizontal section of the dam

In this paper, the parabolic conic function is employed to design the dam geometry on horizontal sections based on Table 1, as follows. By placing the values of design variables in the main geometrical parameters' vectors, the horizontal section is obtained at any height. Fig. 1. illustrates the diagram of arch dam geometrical design equations.

Table 1. Arch dam geometrical design equations

	Mathematical equation of arch dam design	Quantification	Fig.
	Crown cantilever shape		
Elliptic conic function	$F(Y,Z) = aY^2 + bYZ + cZ^2 + dY + eZ + f$	The elliptic conic functions	
	$V = \begin{bmatrix} Z_1 & Z_6 & Z_9 & Z_{12} & Z_{16} \\ Y_1 & Y_6 & Y_9 & Y_{12} & Y_{16} \end{bmatrix}$	Determination the constant coefficients of the conic function using the matrix of definite coordinates (V matrix)	1-a
	$U_W(Z) = \frac{-(bZ+d) + \sqrt{(bZ+d)^2 - 4a(cZ^2+eZ+f)}}{2a}$	Determining the upstream projection at any height using the root of the conic function	
	$DU_W(Z) = \frac{-b + [b(bZ+d) - 2a(2cZ+e)][(bZ+d)^2 - 4a(cZ^2+eZ+f)]^{-0.5}}{2a}$	Temporarily determining the tangent point location on the upstream face of the cantilever with a derivate of the root function	1-b
	$DU_W(Z_{16}) = \frac{-b + [b(bZ_{16}+d) - 2a(2cZ_{16}+e)][(bZ_{16}+d)^2 - 4a(cZ_{16}{}^2+eZ_{16}+f)]^{-0.5}}{2a}$	Maximum offset on	

		water front by locating the crest level	
	$tan^{-1}(DU_w(Z)) = \theta_{CrestUS}$	Determining maximum upstream slope	1-c
	$US(Y) = \frac{-(bY+e) \pm \sqrt{(bY+e)^2 - 4c(cY^2+dY+f)}}{2C}$	The curve above (+) and below (-) the tangent point	1-b
	Y (Z, Downstream) = Y (Z, Upstream) + t_c (Z)	The curve of the downstream face of the crown cantilever	
Thickness of arch dam			
3rd degree polynomial	$t_c(z) = a_0 + a_1 z + a_2 z^2 + a_3 z^3$	$t_c(z)$: Crown thickness	1-f
	$t_{AL}(z) = b_0 + b_1 z + b_2 z^2 + b_3 z^3$	$t_{AL}(z)$: Left abutment thickness	1-f
	$t_{AR}(z) = c_0 + c_1 z + c_2 z^2 + c_3 z^3$	$t_{AR}(z)$: Right abutment thickness	1-f
Radius of curvature			
Cubic spline	$R_{UL}(Z) = d_0 + d_1 Z + d_2 Z^2 + d_3 Z^3$	$R_{UL}(z)$: Radius of left water face	
	$R_{UR}(Z) = e_0 + e_1 Z + e_2 Z^2 + e_3 Z^3$	$R_{UR}(z)$: Radius of left face right	
	$R_{DL}(Z) = f_0 + f_1 Z + f_2 Z^2 + f_3 Z^3$	$R_{DL}(z)$: Radius of air face left	
	$R_{DR}(Z) = g_0 + g_1 Z + g_2 Z^2 + g_3 Z^3$	$R_{DR}(z)$: Radius of air face right	
Horizontal arches			
Parabolic conic functions	$y = US + \frac{(x_e)^2}{2R_U}$	Water face	1-d 1-e
	$y = DS + \frac{(x_i)^2}{2R_D}$	Air face	1-d 1-e
	$t_a(x) = t_C + \frac{(x-x_{ed})^2 (t_A - t_C)^2}{(x_e - x_{ed})^2}$ $x_{ed} < x < x_e$		1-f
	$t_a = t_C$ $x < x_{edL}$		1-f

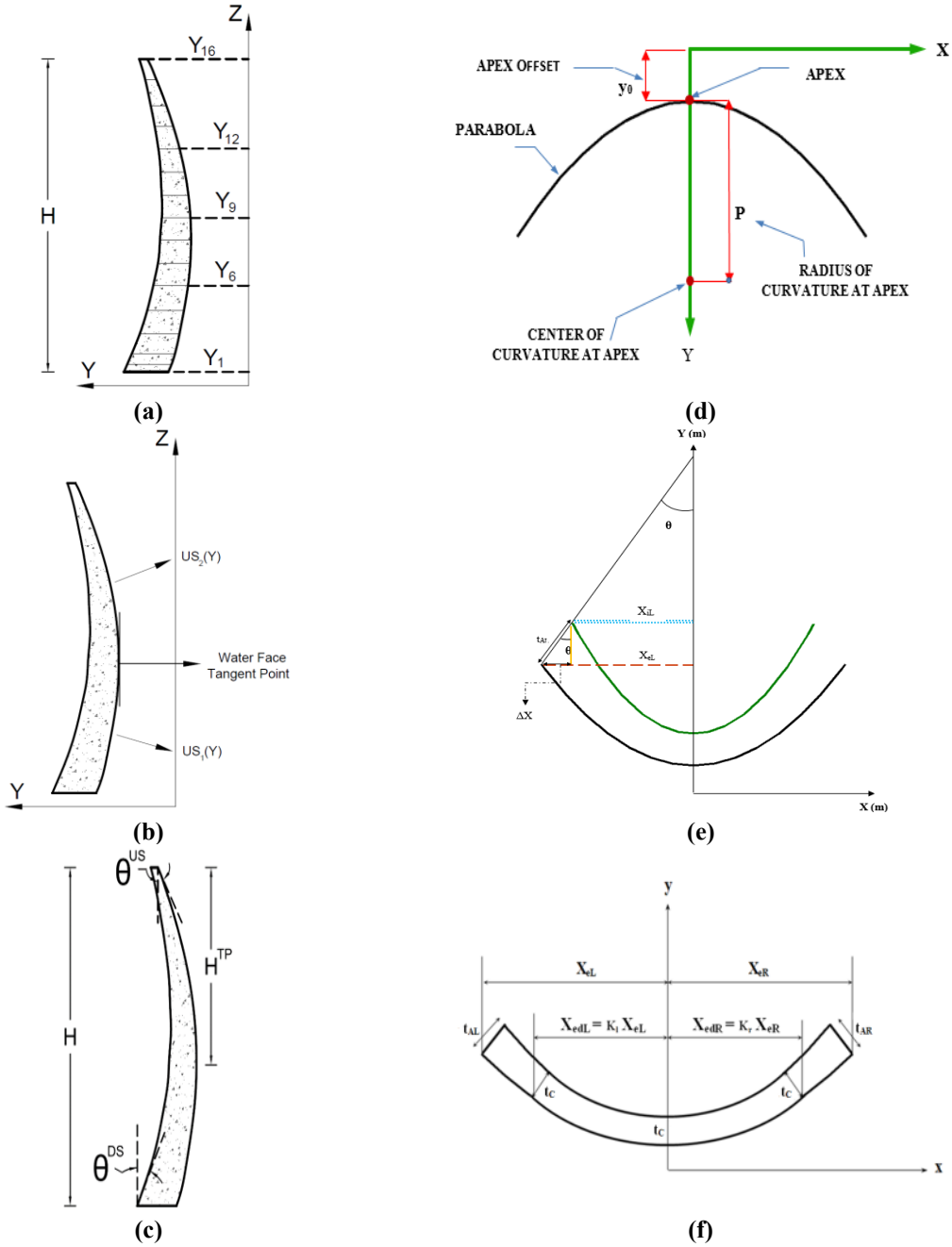


Figure 1. Parameters defining dam shape
a) View of Matrix V (Points are selected at dam base, 0.26 H, 0.49H, 0.72H and dam crest, respectively.)
b) Two-segment ellipse of upstream face
c) Maximum slope of overhang at the upstream and downstream faces
d) Parabola definition
e) Water and air faces in horizontal arch section
f) Horizontal arch of the dam body at elevation

2.3 Analysis and verification of finite element model

The program written using the design variables' vector can automatically produce the finite-element model. The outer surfaces of the foundation are considered to be parallel to the main coordinate system. The constraint of nodal displacement is applied to nodes on the lateral surfaces and the bottom of the foundation. The dimensions of the foundation along the stream and cross stream are three times the width of the valley, and its depth is twice the height of the dam body, as depicted in Fig. 2. The height of the dam body and the width of the valley at the level of dam crown respectively equal 325 and 446 in meter. The generated model includes the dam and foundation as seen in Fig. 3. The finite element model was discretized in thickness by two layers of isoparametric 20-node brick elements. The physical and mechanical properties required for finite-element modeling of dam body and foundation are presented in Fig. 2.

Loads applied to the dam include the dam body weight and hydrostatic pressure. Two load combinations are considered in shape design of arch dam; One is UNS loading related to the unusual static load, including stage construction, and the other is the US load combination related to the loading of stage construction and the hydrostatic pressure of the normal level of reservoir water. In US loading, the model will undergo static analysis for (stages of concreting + 1) times. Eight concreting stages are considered for the simulation of the construction process. The ninth structural analysis is related to the upstream hydrostatic pressure performed on the deflected dam body under its own weight.

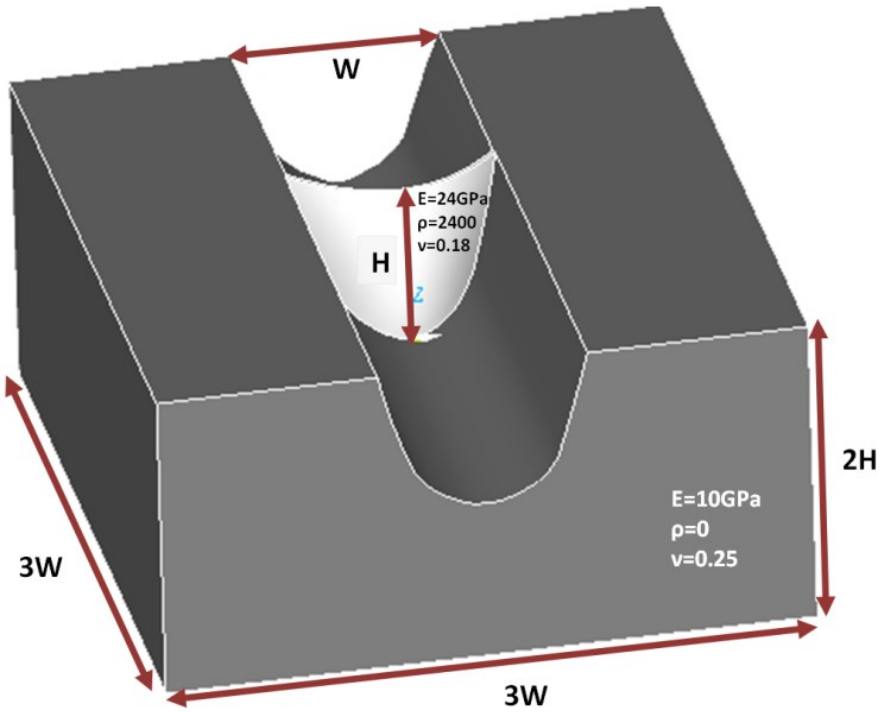


Figure 2.Dimensions of the numerical model and the mechanical properties of the structure

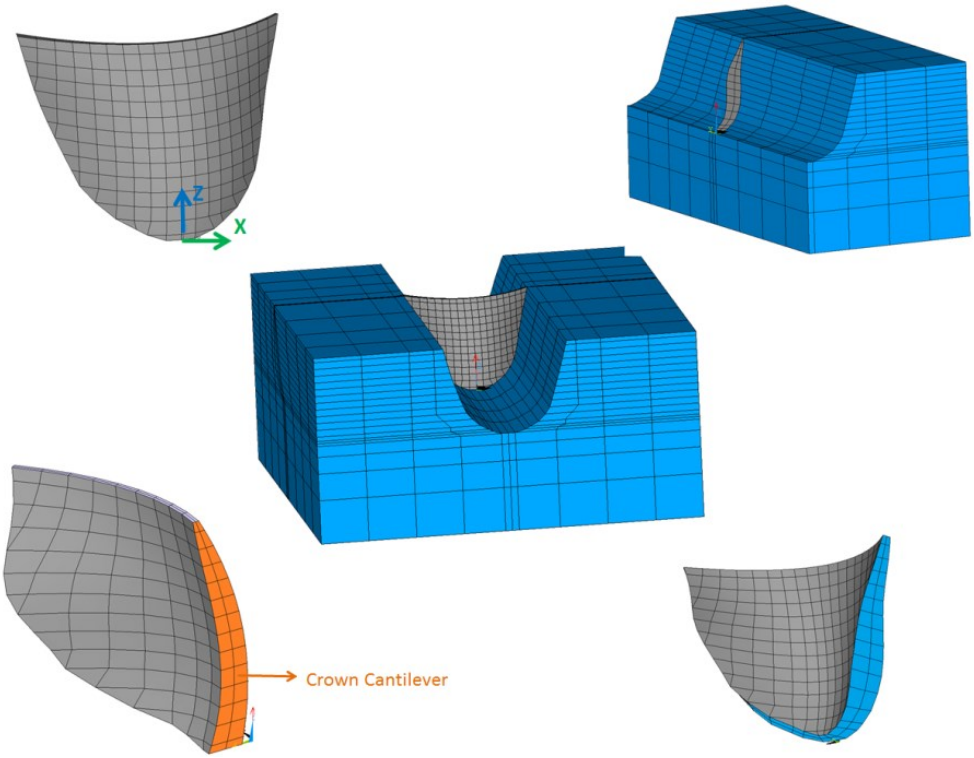


Figure 3.Dam- Foundation Model considered in discretization

The hydrostatic pressure of the normal level of the reservoir is shown in Fig. 4. The hydrostatic pressure applied to the upstream face is perpendicular to the surface of each element [17]. On the left side of the noted Figure, the contour of the hydrostatic pressure is visible. To verify the application of reservoir water on the upstream, the equation of hydrostatic pressure can be controlled. By dividing the hydrostatic pressure of the central crown cantilever base level by $\gamma_w = 9.80$, the height of the upstream water is obtained equal to 315 m.

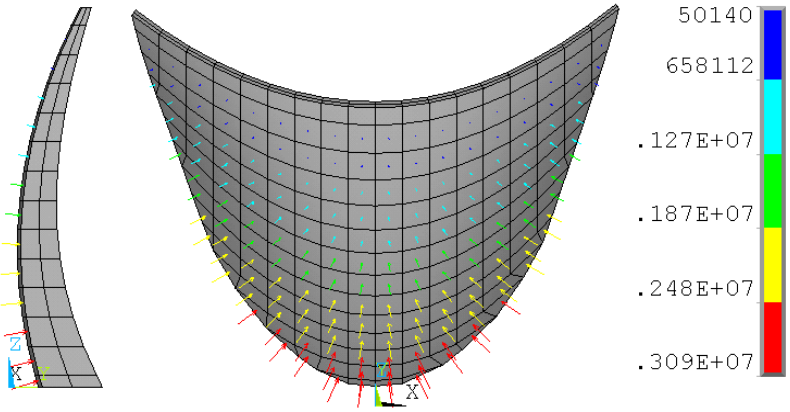


Figure 4.Hydro-static pressure in US face of dam body in normal water level

2.3.1. Stage construction

The structure of the dam consists of vertical blocks, which are connected to one another during dam construction by a grout with a low tensile strength. In other words, they turn the dam structure which used to perform in the form of a statically determined cantilever into an integrated structure with a high statically indeterminacy degree. If the dead load in structural analysis is applied at one, it leads to fictitious stress. Therefore, it is necessary to consider stage construction in the static analysis, and it must also be considered in the optimization of the shape of concrete arch dams [1,7-8,11,14,18-24]. The distribution of stress under dead load would be erroneous if stage construction modeling is not considered. To model an actual number of concreting stages, a large number of computations steps may be needed. In this study, modeling is performed through 8 concreting stages. This is a simplified assumption. Fig. 5 depicts the steps of concreting used in the static analysis.

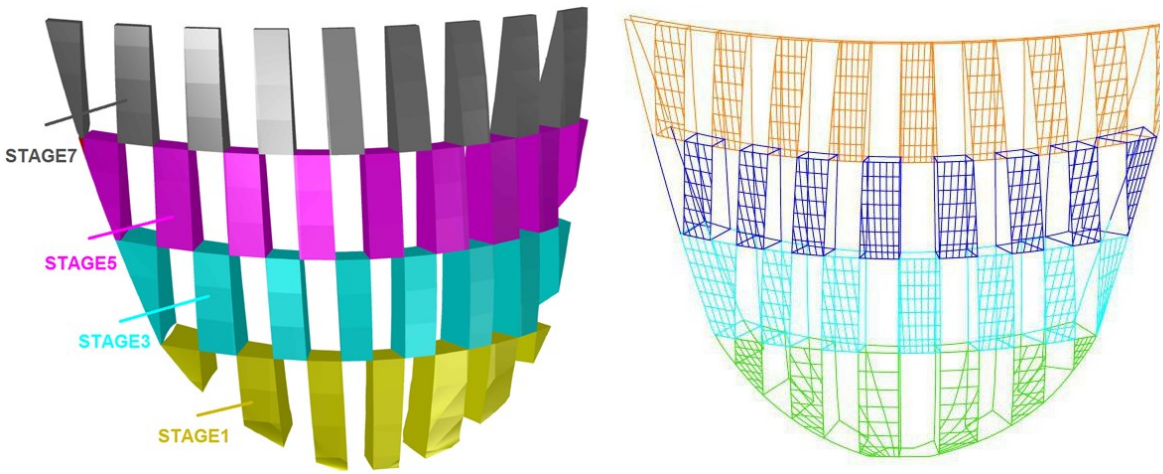


Figure 5.Sequential construction of dam body with eight stages

2.3.2. Validation of the finite-element model

Model validation is conducted using the finite-element software used in this study as well as the ABAQUS software. Table 2 presents the values of natural frequencies for the first four vibration modes obtained by the two programs. The obtained frequencies are compatible with each other. The symmetry and asymmetry of the shape of the first four vibration modes in the two programs are appropriately compatible as illustrated in Fig. 6. Moreover, the dominant mode along the stream (mode 2) and cross stream (mode 4) is shown for both programs. The Mechanical ANSYS software utilized for structural analysis in this paper. The ABAQUS software utilized to validation purpose only.

Table 2. Modal frequencies of FEM model

Mode Number	Shape of mode		Natural Frequency (Hz)	
	ANSYS	ABAQUS	ANSYS	ABAQUS
1	Asymmetric	Asymmetric	1.65	1.53
2	Symmetric	Symmetric	2.08	2.03
3	Symmetric	Symmetric	2.81	2.69
4	Asymmetric	Asymmetric	3.11	3.05

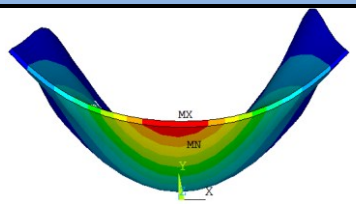
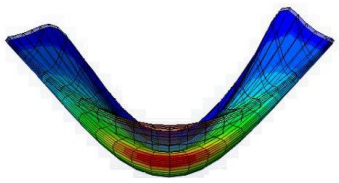
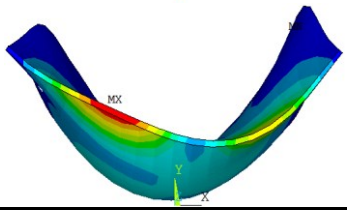
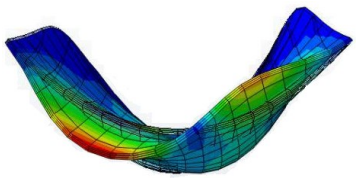
Mode Number	Direction and type of Dominant mode	Shape of mode	
		ANSYS	ABAQUS
2	Stream (Symmetric)		
4	Cross- Stream (Asymmetric)		

Figure 6. Comparison of dominant modes of model in different FE codes

3. Optimization of the arch dam and optimization strategy

While employing all physical, mechanical, and geometrical features of the design, the optimization problem must be able to present the behavior of the structure against applied loads by considering all design constraints in order to achieve an appropriate design. In the Eq. (1), the standard form of the optimization problem used in this study is demonstrated [25]. In this study, the objective function is considered in the form of the weighted linear combination of two functions of cost and safety.

$$\begin{aligned} &Find: X \\ &Minimize: F(X)^{SPSA} = \omega_1 \times f_1^{Normalized} + \omega_2 \times f_2^{Normalized}; \\ &\omega_1 + \omega_2 = 1; \\ &Subject, to: g_i(X) \le 0; \\ &X^L \le X \le X^U \end{aligned} \tag{1}$$

In the above equation, the objective functions must be scale less and having the same order so that the criteria with different scales (cubic meter and Pascal) can be compared. In the present study, the fuzzy normalization method which belongs to criteria which must be minimized is used based on the Eq. (2):

$$\begin{aligned} &f_K^{\,Normalized} = \frac{f_K - f_K^*}{f_K^- - f_K^*}; \\ &K = 1,2 \end{aligned} \tag{2}$$

Where f_K^- and f_K^* is respectively the minimum and maximum values of the K^{th} objective function and their values are obtained through trial and error. By normalizing the objective functions, they will have positive and normalized values with the maximum value of 1.

3.1. Optimization strategy

A program is written using MATLAB in order to generate the coordinates of all nodes required for the finite-element model of the dam body. To produce nodes placed on horizontal and vertical arches, the equations noted in Table 1 are utilized. In the optimization process, geometrical, stress, and stability constraints are considered in the form of penalty function. Fig. 7 illustrates the flowchart of the optimization process. The algorithm is executed and the constraints are controlled in MATLAB. ANSYS is utilized only to analyze the structure and extract the stress values in dam elements and the volume of dam body. ANSYS code invoked by MATLAB in each iteration of optimization.

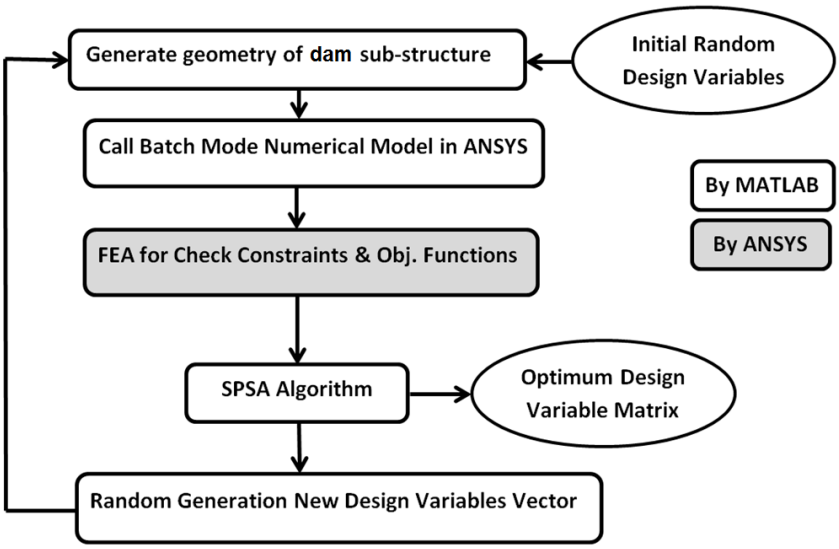


Figure 7. Flowchart of MATLAB and ANSYS interactive optimization

3.2. SPSA optimization algorithm

The SPSA gradient based algorithm is a powerful algorithm for optimizing complex system, developed by Spall (1994) [26]. A feature of this algorithm is that, in each optimization iteration, it requires only twice evaluating the objective function (structural analysis), independent of the number of design variables. The random nature of this algorithm increases the probability of reaching the global optima.

Execution of SPSA algorithm includes 5 steps, demonstrated in the flowchart in Fig. 8: [7]. In this algorithm, $F(X)^{SPSA}$ is introduced as the objective function.

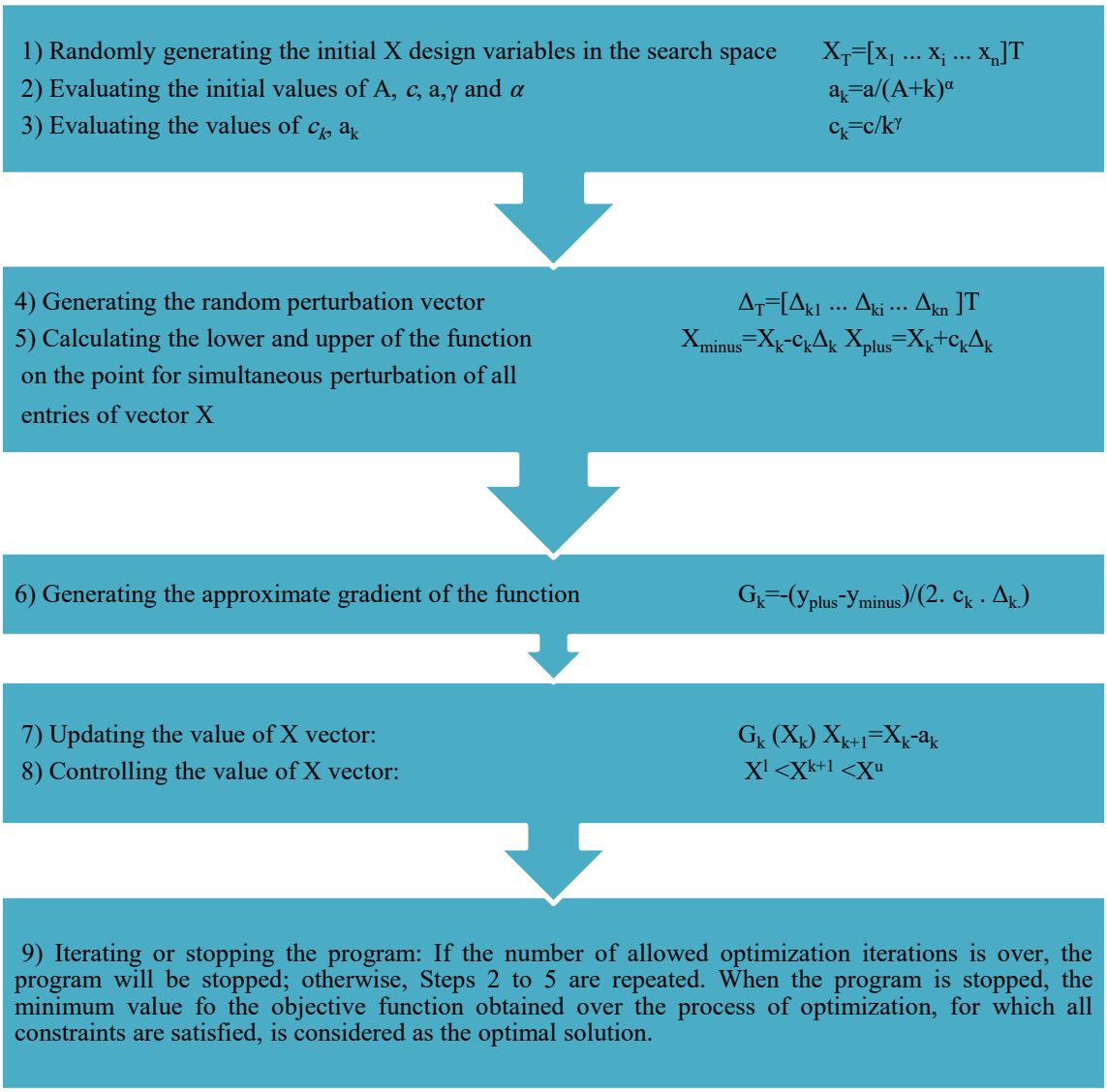


Figure 8.The flowchart of SPSA algorithm

3.3. Design variables

Design variables are those used for the description and determination of the dam geometry. In optimization of the shape of arch dams, 33 design variables based on Fig. 9 are utilized in the optimization model.

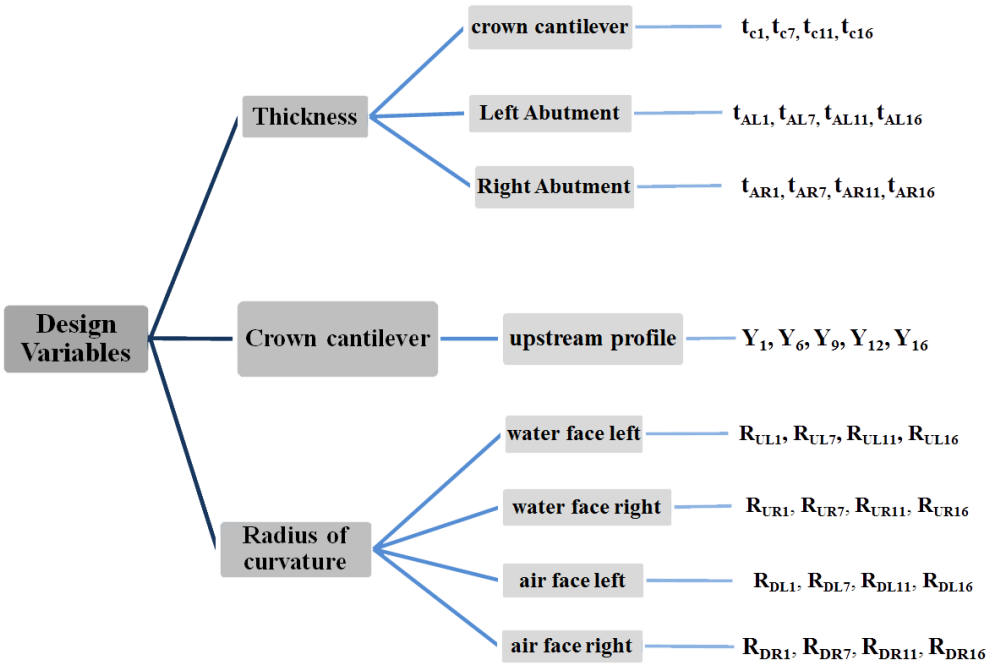


Figure 9. The diagram of design variables

3.4. Objective functions

In analysis and design of concrete dam body the stress and deflection limit states are considered by the designers. The concrete gravity dams, as statically determinate cantilever beams, can have significant deflections, but in concrete arch dams, because of its high statically indeterminacy nature, often have insignificant deflection in the river direction. The drift limit state for very stiff structures such as concrete dams has been taken equal to 0.02%, which is often satisfied for arch dams [17, 27]. The first objective function is the volume of concrete used for building the dam body which indicates the cost criterion. The second objective function is the maximum principal stress, indicating the safety criterion. As dams are constructed using unreinforced concrete, they have little resistance to tensile stress. Thus, designers of arch dams try to reduce maximum tensile stress of dam body dam by changing their shapes. In the Eq. (3), i refers to the number of elements, limited to N which, in the present study, equals total elements in the arch dam body, i.e., 392.

$$f_1 = \sum_{i=1}^{N} V_i$$
$$f_2 = max(S_1^1.S_1^2.,,,.S_1^N) \quad (3)$$

3.5. Constraints

In the optimization of the arch dam, optimization constraints are categorized into three groups of geometrical, stress, and stability, based on Table 3. (Engineer Manual 110-2-2201, 1994) Moreover, bounds constraints are depicted in the final section (Section 5.)

Table 3. Constraints Definition

	Constraint functions $g_i(X)$	Quantification	Fig.
Geometrical constraints	**Thickness of horizontal arch**		
	$T_{C_{i+1}} < T_{C_i} \Rightarrow \frac{T_{C_{i+1}}}{T_{C_i}} - 1 \leq 0 \quad (i = 1,2,\dots,n-1)$	Reduced thickness of the crown cantilever from the base to the crown of the dam.	1-a
	$T_{C_i} < T_{AL} \Rightarrow \frac{T_{C_i}}{T_{AL}} - 1 \leq 0 \quad (i = 1,2,\dots,n)$ $T_{C_i} < T_{AR} \Rightarrow \frac{T_{C_i}}{T_{AR}} - 1 \leq 0 \quad (i = 1,2,\dots,n)$	Smaller thickness of the crown cantilever from the right and left abutments at any height.	1-f
	Slope of overhang in upstream and downstream of arch dam		
	$\theta_{max} \leq \theta_{alw}$	Smaller maximum angle between the slope tangent to the curve of upstream and downstream faces of the crown cantilever with the z axis in the crown and base of the dam compared to its allowable value (0.6 in the upstream and 0.4 in the downstream).	1-c
	Crown cantilever profile		
	$Y_{i+1} < Y_i \Rightarrow \frac{Y_{i+1}}{Y_i} - 1 \leq 0 \quad (i = 1,2,\dots,n_{\text{tangentpoints}})$ $Y_i < Y_{i+1} \Rightarrow \frac{Y_i}{Y_{i+1}} - 1 \leq 0 \quad (i = n_{\text{tangentpoints}},\dots,n)$	Decreasing trend of the upstream and downstream projection of the crown cantilever up to the tangent points and the increasing trend of these values from the tangent point to the crown of the dam. The "n" is the total number of dam levels.	1-a
	$H_{\text{Tangentpoint}} < H_{Tangentpoint_{max}} \rightarrow \frac{H_{\text{Tangentpoint}}}{H_{Tangentpoint_{max}}} - 1 \leq 0$	Less distance between the tangent point in the upstream and the dam crown compared to its maximum point (0.6 of dam height).	1-c
	$R_{D_i} < R_{U_i} \Rightarrow \frac{R_{D_i}}{R_{U_i}} - 1 \leq 0 \quad (i = 1,2,\dots,n)$ $R_i < R_{i+1} \Rightarrow \frac{R_i}{R} - 1 \leq 0 \quad (i = 1,2,\dots,n)$	Smaller values of downstream radius of curvature compared to the upstream face along the dam height. Reduced values of radius of curvature from the base to the dam crest.	1-e
Stress	$(S_1)_{i,j} \leq \frac{f_t^{allowable}}{SF_j} (i = 1,2,\dots,Number.of.Elements)$ $(S_1 = First\ Principal\ Stress) \quad SF_{US,UNS} = 1$ $(S_3)_{i,j} \leq \frac{f_c^{allowable}}{SF_j} (j = 1,2,\dots,Number.of.LaodCombination)$ $f_t^{allowable} = 0.324(f_c^{allowable})^{2/3}$ [Raphael,1984]	Smaller maximum stress caused in the dam body under loads than the allowable stress.[28]	
Stability	$1 - \frac{\varphi}{90} \leq 0 \quad , \quad \frac{\varphi}{110} - 1 \leq 0 \quad , \quad 90 < \varphi < 110$	Limitation of the central angle of the dam at height levels of dam to control dam body stability.	

4. Results of the sum-weighted optimization using SPSA algorithm

The set of optimal solutions in the objective space is called a Pareto front. The Pareto front for the optimization problem is presented in Fig. 10. The horizontal axis demonstrates the first objective function, i.e., the volume of concreting the vertical axis of maximum tensile stress (1st principal stress in ANSYS code) of the dam body. To extract the Pareto front, 10 pairs of weight coefficients of $(w_1,w_2)_1,(w_1,w_2)_2,...,(w_1,w_2)_{10}$ are assigned, and then the optimization algorithm is executed. One point of the Pareto front is obtained by each execution of the program, and for the depicted front, 10 separate executions are needed. By changing the weights in the minimization problem, various points of the convex Pareto front are obtained. The time of executions the program is about 16 hours for obtaining each optimal solution using the weighted method (Table. 4). According to the technical literature of shape optimization of concrete arch dams and arch bridges with SPSA optimization algorithm [7,8,23,14,29] and also trial and error in converging the pseudo-objective function $(F(X)^{SPSA})$, the value of maximum iteration number was selected. Therefore, criterion for stopping the iteration of the optimization algorithm is selected 3000 iterations. So, in the present paper the number of structural analysis in order to cost function evaluation and development of Pareto front is 60000 times. Respectively$\frac{1}{3}$ and $\frac{2}{3}$ of the time of each iteration belongs to node generation in MATLAB and the batch mode structural analysis of the finite-element software.
Alternative B is the preferred solution in terms of cost minimization, while Alternative J is the preferred solution in terms of safety criterion.

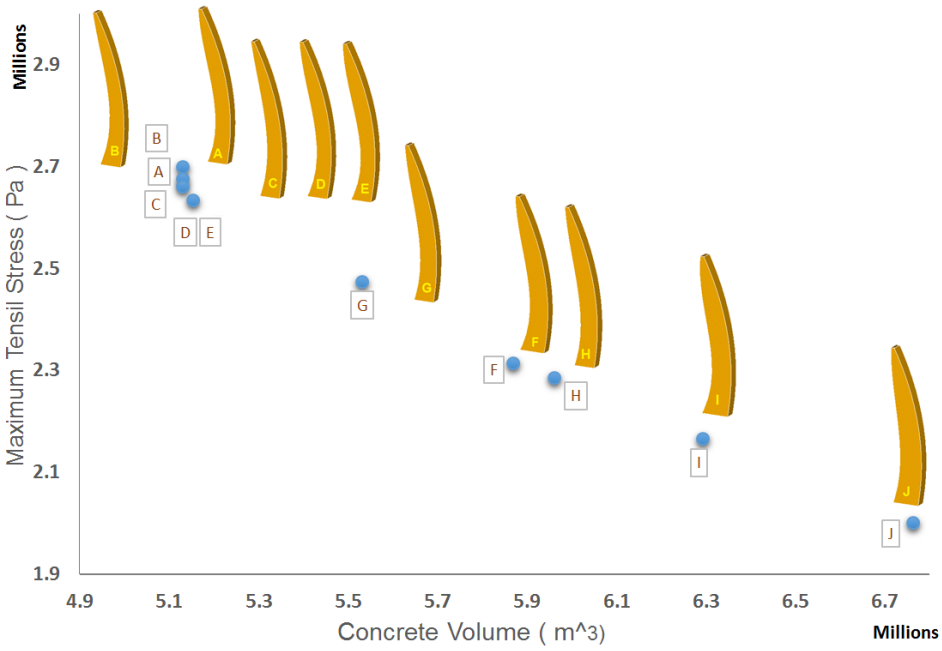
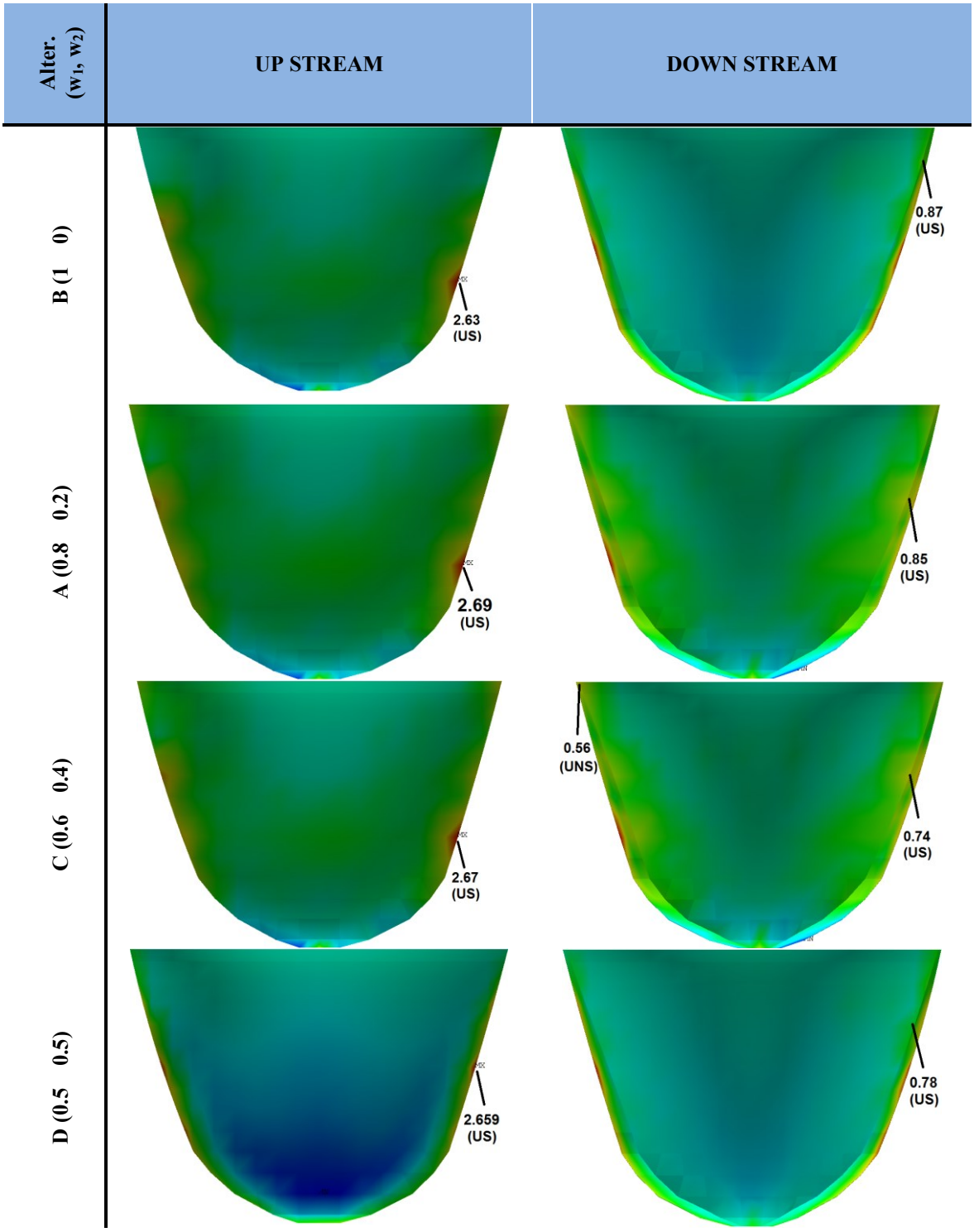
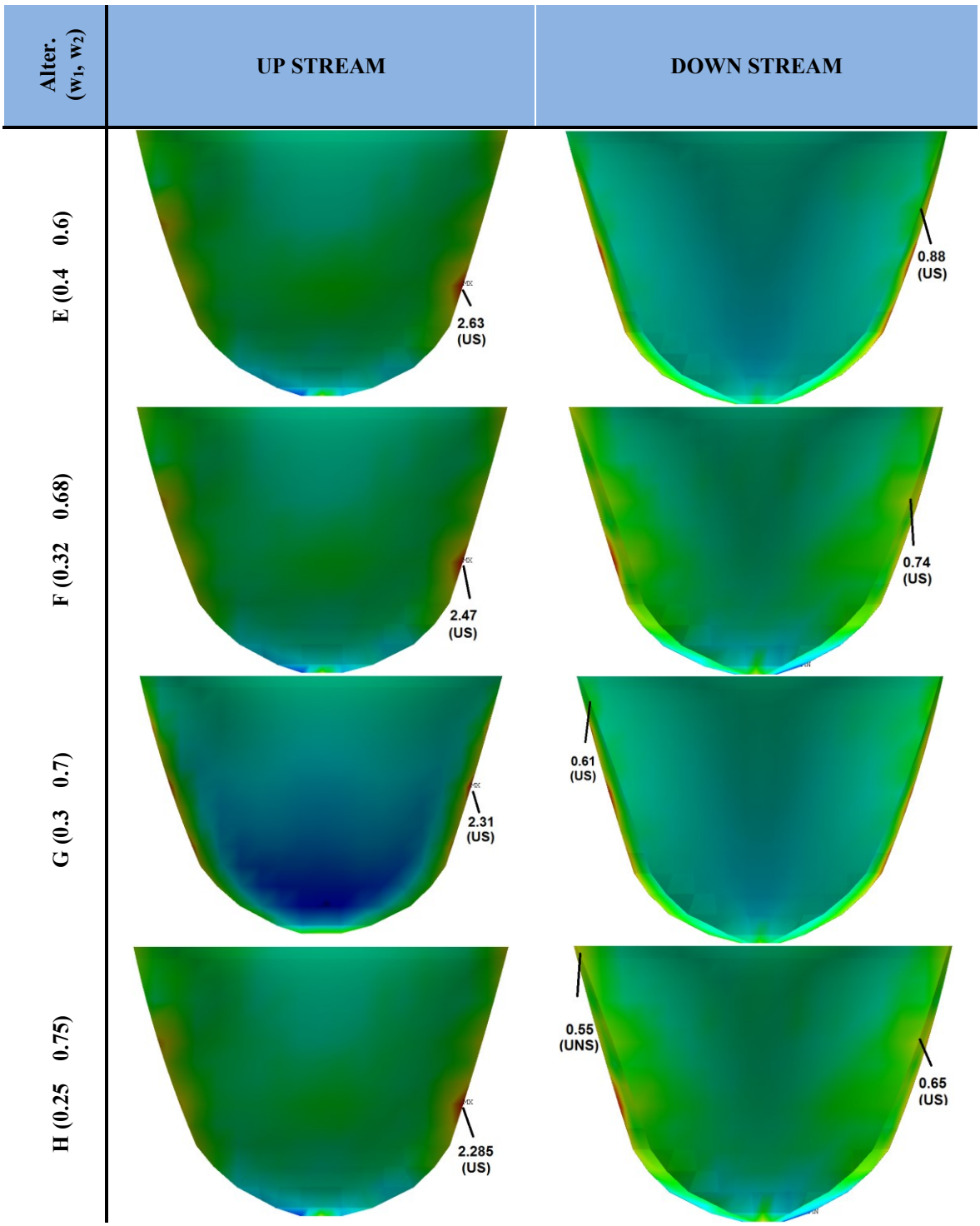


Figure 10. Pareto front using the fuzzy normalized weighting method

The purpose of the Fig. 11 is showing the location and value of the maximum principal stress in dam body in the both sides of dam for all Pareto front alternatives. In Fig. 11, maximum principal stress on upstream and downstream faces are shown. It is clear that, in all optimized

shapes (A-J Alternatives) of the dam, maximum tensile stress is produced under the US load combination in the right abutment of the upstream face.




Alter. (w1, w2)
UP STREAM
DOWN STREAM
E (0.4 0.6)
F (0.32 0.68)
G (0.3 0.7)
H (0.25 0.75)
2.63 (US)
0.88 (US)
2.47 (US)
0.74 (US)
2.31 (US)
0.61 (US)
2.285 (US)
0.55 (UNS)
0.65 (US)

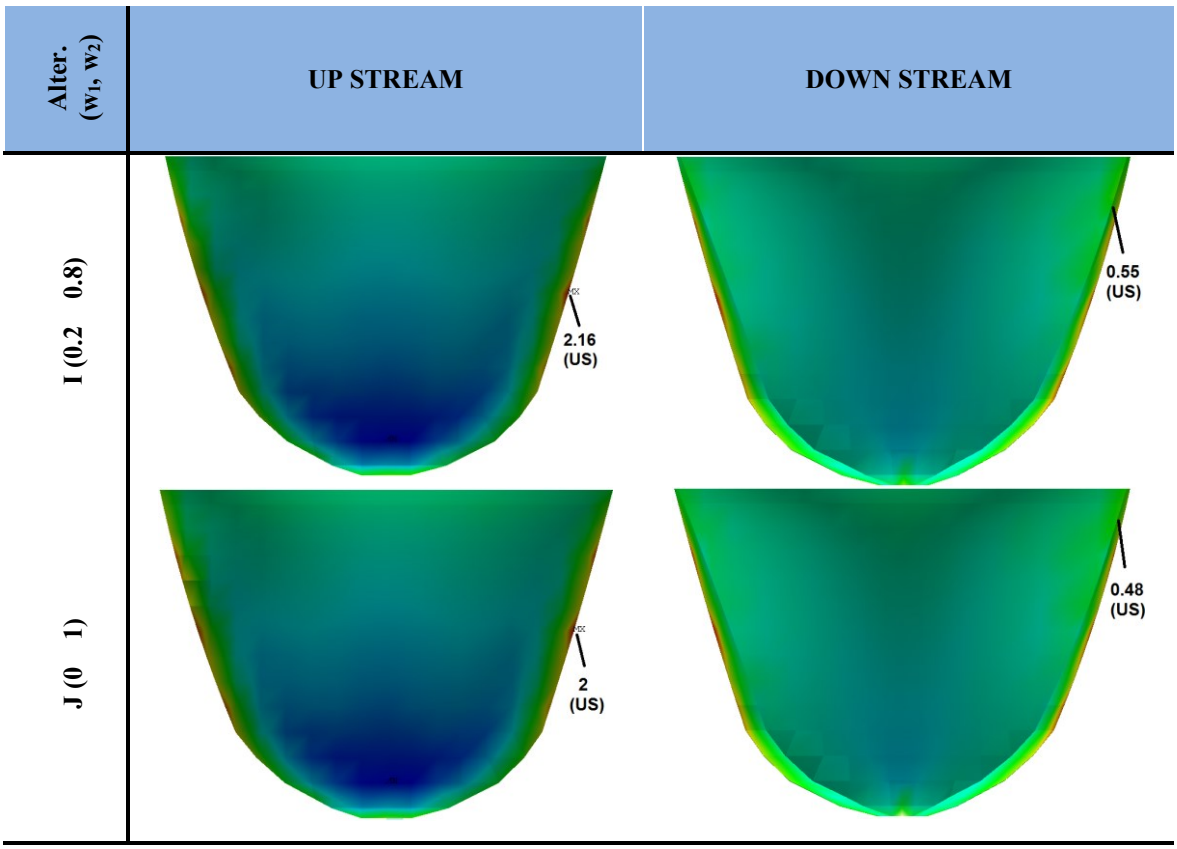


Figure 11. Stress distributions in DS & US faces of optimum alternatives (MPa)

Table 5 presents a summary of results of solving the bin-objective problem of the shape of the arch dam using the weighted method.

Table 4. Evaluating the performance of the optimization algorithm

Comparative points	S.W.SPSA
Number of optimum designs Front	10
Number of estimations of objective functions required in each iteration of the algorithm	2
Number of estimations of the objective functions (structural analysis) needed to generate the entire front	10*3000*2=60000
Time of executing each algorithm (generation of analysis node, control of constraints) (minute) using a Pentium computer	0.32
Time required for developing an optimum design (hour)	$\frac{0.32 * 3000}{60} = 16$
Time required for developing the entire front (hour)	10*16=160
System: ASUS N551jx, Intel(R) Core(TM) i7-4720HQ CPU@2.6GHz, 8G Ram	

Table 5. Compromise solutions of the arch dams optimized using the weighted-sum method

Alter.	ω_1	ω_2	$V(\times 10^6), m^3$	$\sigma_1(\times 10^6), Pa$
B	1.00	0.00	5.1310	2.6330
A	0.80	0.20	5.1530	2.6990
C	0.60	0.40	5.1305	2.6740
D	0.50	0.50	5.1320	2.6590
E	0.40	0.60	5.1540	2.6320
G	0.30	0.70	5.8690	2.3139
F	0.32	0.68	5.5320	2.4730
H	0.25	0.75	5.9620	2.2850
I	0.20	0.80	6.2920	2.1640
J	0.00	1.00	6.7630	2.0000

5. Selecting the preferred solution from the Pareto front using the VIKOR method

The VIKOR method is explained below. This method has a mathematical basis and helps decision makers in their decision making. Refer to (Opricovic and Tzeng, 2004) Reference for further study.

J is the number of alternatives shown with a_1, a_2, …, a_j. For alternative a_j, ranking of the i^{th} criterion is shown with f_{ij} that is, $f_{ij}$is the value of the i^{th} criterion for the alternative a_j. n shows the number of criteria. In present study j and n are 10 and 2 respectively. In VIKOR method, the values of S_j and R_j are obtained based on Eqs. (4) and (5), respectively.

$$S_j = \sum_{i=1}^{n} \left[w_i \frac{f_i^* - f_{ij}}{f_i^* - f_i^-} \right] \tag{4}$$

$$R_j = max_i \left[w_i \frac{f_i^* - f_{ij}}{f_i^* - f_i^-} \right] \tag{5}$$

Where w_i is the weights or coefficients of the i^{th}criterion, expressing the decision maker's preference as the relative importance of the criteria in multi-objective decision-making Values of $S_j$and R_j are used to determine the measure of ranking. As is illustrated in Fig. 12, the ideal point is represented by $F^*$and compromise solution point is represented by F^j.

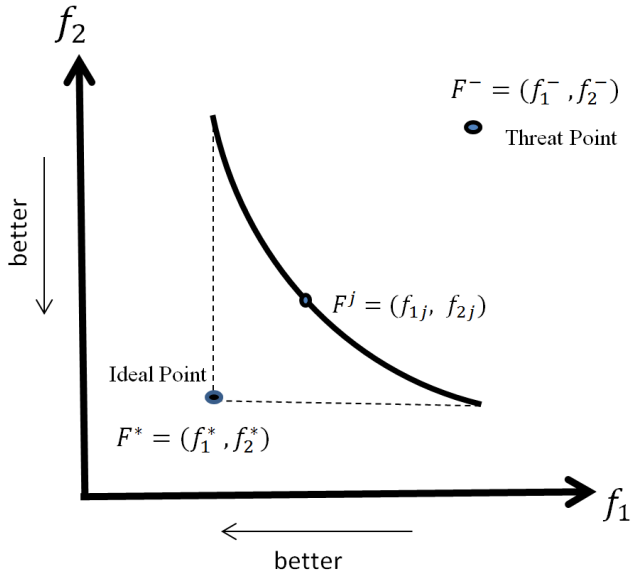


Figure 12. Definition of threat points and ideal points in the Pareto front

The compromise ranking algorithm has the following steps:
Step 1: Determine the best (f_i^*) and the worst (f_i^-) values of all n criteria.
Step 2: Compute the values S_j, and $R_j$by the Eqs. (4) and (5).
Step 3: Compute the VIKOR index (Q_j), by the Eq. (6):

$$Q_j = v\left(\frac{S_j - S^*}{S^- - S^*}\right) + (1-v)\left(\frac{R_j - R^*}{R^- - R^*}\right)$$
$$S^* = min_j\, S_j\,; S^- = max_j\, S_j \qquad (6)$$
$$R^* = min_j\, R_j\,; R^- = max_j\, R_j$$
$$assume: v = 0{,}5$$

Step 4: Rank the alternative, by sorting the values S, R and Q in an increasing order.
Step 5: Propose an alternative as a compromise solution (having the minimum value), that is the best ranked by the measure Q in the three ranking lists of S, R and Q, if the following two conditions are satisfied:
Condition1: if alternatives $a'$and a'' are the first and second compromise solution respectively in the ranking list Q, and j represents the number of alternatives, the Eq. (7) is satisfied. In the present research, the value of $DQ$is 0.0111.

$$Q(a'') - Q(a') \geq DQ$$
$$DQ = \frac{1}{j-1} \qquad (7)$$

Condition2: alternative $a^{'}$ must also be the best ranked by S and/or R. If condition 1 is not satisfied, then a set of compromise solutions is proposed from among $a^{'}, a^{''}, \ldots, a^{(m)}$, where maximum m is determined based on Eq. (8).

$$Q(a^{''}) - Q(a^{'}) \leq \frac{1}{j-1} \tag{8}$$

If condition 2 is not satisfied, then alternatives $a^{'}$ and $a^{''}$ are proposed as compromise alternatives.

In what follows, preferred solutions are obtained from among 10 non-dominated solutions using the program written in Excel for the VIKOR method, various weights are examined for objective functions in two states. In the first state, weight factors of the cost of dam construction and the dam safety criterion are considered equal to 1. In Fig. 13, the process of computation of the written program for ranking using the VIKOR method is demonstrated. As shown by the values of VIKOR (Q) in Fig. 13, the preferred solution (G) are obtained. Moreover, for the state in which the weight factor of the first criterion is 2 and that of the second criterion is 1, a set of 7 solutions (A, B, C, D, E, F, G) is obtained (Fig. 14).

	A	B	C	D	E	F	G	H	I	J	K	L
1		Criteria	Name	f1	f2							
2				Volume	Sigma 1				w1	w2		
3			Unit	10^6 m^3	10^6 Pa				1	1		
4	Performance matrix		Exterm	Min	Min		S1	S2	S	R=MAX(S1,S2)	Q	
5		Alternatives	B (1,0)	5.131E+06	2.63E+06		0.000	0.906	0.907	0.906	0.433	
6			A (0.8.2)	5.153E+06	2.70E+06		0.014	1.000	1.014	1.000	1.0000	
7			C (0.6,0.4)	5.131E+06	2.67E+06		0.000	0.964	0.964	0.964	0.7415	
8			D(0.5,0.5)	5.133E+06	2.66E+06		0.001	0.944	0.945	0.944	0.639	
9			E(0.4,0.6)	5.155E+06	2.63E+06		0.015	0.905	0.919	0.905	0.489	
10			G(0.3,0.7)	5.869E+06	2.31E+06		0.452	0.450	0.903	0.452	0.000	1
11			F(0.32,0.68)	5.533E+06	2.47E+06		0.246	0.678	0.924	0.678	0.300	
12			H(0.25,0.75)	5.963E+06	2.29E+06		0.510	0.408	0.918	0.510	0.120	
13			I(0.2,0.8)	6.292E+06	2.16E+06		0.711	0.234	0.946	0.711	0.430	
14			J(0,1)	6.764E+06	2.00E+06		1.000	0.000	1.000	1.000	0.937	
15	i	2										
16	j	10										
17	v	0.5										
18	f1*=min(f1(j))	5.1E+06										
19	f2*=min(f2(j))	2.0E+06										
20	$f_1^- =$ MAX(F1(j))	6.8E+06										
21	$f_2^- =$ MAX(F1(j))	2.7E+06										
22	DQ=1/(j-1)	0.1111111										
23	S*=MIN(Sj)	0.903										
24	$S^-=$ MAX(Sj)	1.014										
25	R*=MIN(Rj)	0.452										
26	$R^-=$ MAX(Rj)	1.000										

Figure 13. The VIKOR program written in Excel for equal weights of the objective functions

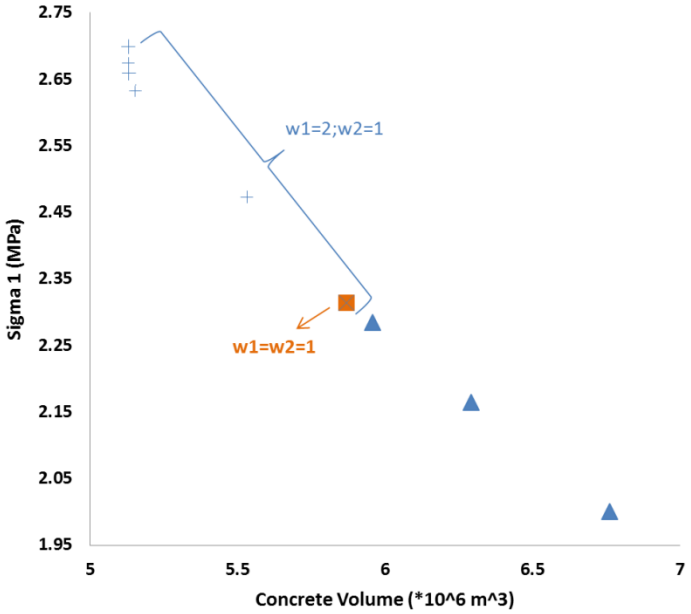


Figure 14. Preferred solutions obtained by VIKOR method

Table 6 presents the vector of design variables of the preferred solution and the bounds constraints defined for the optimization problem. All 33 values of the vector of variables of the optimized design (indicated in Fig. 9) fall in the range of minimum and maximum, demonstrating the correct performance of the optimization algorithm. Moreover, the convergence diagram of the algorithm in 3000 iterations is shown in Fig. 15.

Table 6. The vector of optimal variables and bounds constraints of the preferred solution (G)

	t_{c1}	t_{c7}	t_{c11}	t_{c16}	t_{AL1}	t_{AL7}	t_{AL11}	t_{AL16}	t_{AR1}	t_{AR7}	t_{AR11}
X_U	60	55	45	12	65	70	60	12	65	70	60
X_{OPT}	58.12	45.2	35.2	9.06	60.58	60.4	42.12	10.46	61.25	69.2	55.32
X_L	45	35	25	8	45	55	40	8	45	55	40
	t_{AR16}	Y_1	Y_6	Y_9	Y_{12}	Y_{16}	R_{UL1}	R_{UL7}	R_{UL11}	R_{UL16}	R_{UR1}
X_U	11	25	9	12	32	70	110	125	155	210	110
X_{OPT}	10.3	21.25	6.2	10.6	21.15	69.79	96.34	124.37	129.58	209.9	95.11
X_L	8	15	6	8	19	55	90	105	130	190	90
	R_{UR7}	R_{UR11}	R_{UR16}	R_{DL1}	R_{DL7}	R_{DL11}	R_{DL16}	R_{DR1}	R_{DR7}	R_{DR11}	R_{DR16}
X_U	125	155	210	60	70	105	210	60	70	105	210
X_{OPT}	123.3	146.6	208.21	39.92	51.93	89.22	191.49	42.45	52.91	94.63	207.44
X_L	105	130	190	40	50	85	180	40	50	85	180

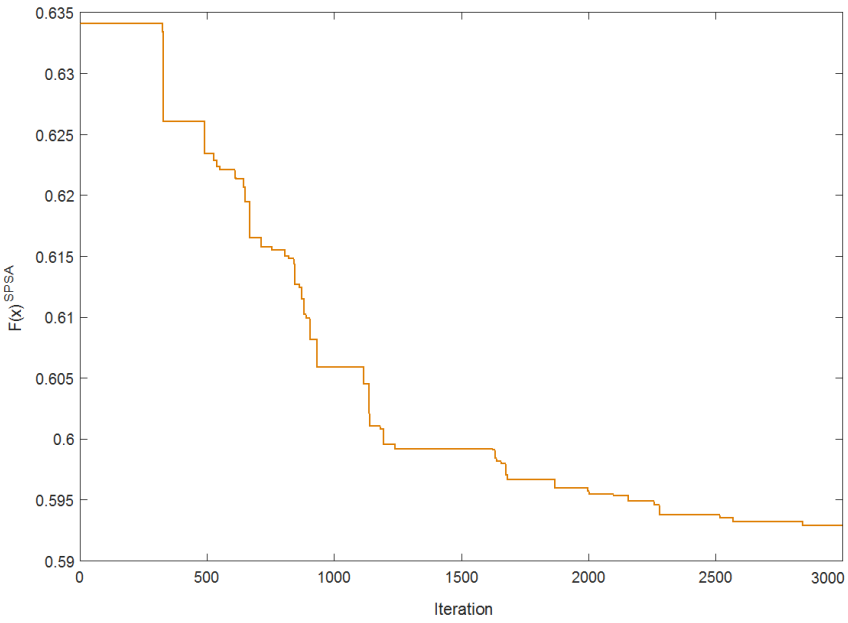


Figure 15. The Convergence Curves for the S.W.SPSA Algorithm

6. Conclusion

The present study examined the process of optimization of the shape of arch dams and selection of preferred solutions from among optimal solutions. The written code established an interaction between two engineering programs, programming software in order to manage the optimization algorithm and a finite-element program for structural analysis. The novelties of this article include the SPSA algorithm in the form of a weighted linear combination method of the objective functions of concrete cost and maximum tensile stress; the consideration of the effect of stage construction of high arch dams in the optimization of arch dams; and utilization of the VIKOR decision-making method for the selection of the preferred solution. The fact that the optimal vector of design variables fall within the range of bounds constraints indicates the accurate performance of the employed algorithm. The proposed optimization process can assist less experienced concrete arch dam designers to design and decide upon the preferred solution from among optimal ones.

References

1. Takalloozadeh M, Ghaemian M (2014) Shape optimization of concrete arch dams considering abutment stabilityScientia IranicaTransaction A, Civil Engineering, 21(4):1297-1308.
2. Akbari J, Ahmadi, MT, Moharrami H (2011) Advances in concrete arch dams shape optimizationApplied Mathematical Modelling, 35(7):3316-3333, https://doi.org/10.1016/j.apm.2011.01.020
3. Fengjie T, Lahmer T (2017) Shape optimization-based design of arch type dams under uncertainties, Engineering Optimization, 50(9):1470-1482, https://doi.org/10.1080/0305215X.2017.1409348

4. Kaveh A, Mahdavi VR (2013) Shape optimization of arch dams under earthquake loading using meta-heuristic algorithmsKSCE Journal of Civil Engineering, 17(7):1690-1699, https://doi.org/10.1007/s12205-013-0463-1
5. Li S, Ding L, Zhao L, Zhou W (2009) Optimization design of arch dam shape with modified complex methodAdvances in Engineering Software, 40(9):804-808, https://doi.org/10.1016/j.advengsoft.2009.01.013
6. Paixão J, Matos DS (2012) SHAPE OPTIMIZATION IN THE DESIGN OF CONCRETE ARCH DAMS-TWO CASE STUDIESBlucher Mechanical Engineering Proceedings, 1(1):4273-4284, https://doi.org/ 10.5151/meceng-wccm2012-19802
7. Pourbakhshian S, Ghaemain M (2016) Shape optimization of arch dams using sensitivity analysis, KSCE Journal of Civil Engineering, 20(5):1966-1976, https://doi.org/10.1007/s12205-015-0135-4
8. Pourbakhshian S, Ghaemian M and Joghataie, A (2016) Shape optimization of concrete arch dams considering stage constructionScientia IranicaTransaction A, Civil Engineering, 23(1):21-35, https://doi.org/ 10.24200/SCI.2016.2094
9. Zhang XF, Li SY, Chen YL (2009) Optimization of geometric shape of Xiamen arch damAdvances in engineering software, 40(2):105-109, https://doi.org/10.1016/j.advengsoft.2008.03.013
10. Meng R, Cheong KH, Bao W, Wong KKL, Wang L, Xie NG (2018) Multi-objective optimization of an arch dam shape under static loads using an evolutionary game method, Engineering Optimization, 50(6):1-17, https://doi.org/10.1080/0305215X.2017.1378876
11. Pouraminian M, Ghaemian M (2017) Multi-criteria optimization of concrete arch dams, 24(4):1810-1820, https://doi.org/10.24200/SCI.2017.4272
12. Sun L, Zhang W, Xie N (2007) Multi-objective optimization for shape design of arch dams, Computational methods in engineering and science, part, 9, https://doi.org/10.1007/978-3-540-48260-4_145
13. Xie NG, Chen Z, Cheong KH, Meng R, Bao W (2018) A Multiobjective Game Approach with a Preferred Target Based on a Leader-Follower Decision Pattern, Mathematical Problems in Engineering, 1-12, https://doi.org/10.1155/2018/7358621
14. Pouraminian, M., & Pourbakhshian, S (2019) Multi-criteria shape optimization of open-spandrel concrete arch bridges: Pareto front development and decision-makingWorld Journal of Engineering, 16(5),670-680, https://doi.org/10.1108/WJE-04-2019-0104
15. Ashrafi, SM (2019) Investigating Pareto Front Extreme Policies Using Semi-Distributed Simulation Model for Great Karun River BasinJournal of Hydraulic Structures, 5(1), 75-88.
16. Opricovic S, Tzeng GH (2004) Compromise solution by MCDM methods: A comparative analysis of VIKOR and TOPSIS European journal of operational research, 156(2):445-455, https://doi.org/ 10.1016/S0377-2217(03)00020-1
17. Pouraminian M, Pourbakhshian S, Farsangi EN., & Fotoukian R (2019) Probabilistic safety evaluation of a concrete arch dam based on finite element modeling and a reliability LR approachCivil and Environmental Engineering Reports, 29(4), 62-78, https://doi.org/10.2478/ceer-2019-0044

18. Alembagheri M (2018) A Study on Structural Safety of Concrete Arch Dams During Construction and Operation PhasesGeotechnical and Geological Engineering, 1-21, https://doi.org/10.1007/s10706-018-0628-2
19. Engineers U.S.AC.o., (1994) Arch Dam Design, Engineering and Design: Arch Dam Design, Engineer Manual EM 1110-2-2201, Washington, DC.
20. Hariri-Ardebili, MA., and Mirzabozorg, H (2011) Reservoir fluctuation effects on seismic response of high concrete arch dams considering material nonlinearityJournal of Civil Engineering Research, 1(1):9-20, https://doi.org/105923/j.jce.20110101.02
21. Hariri-Ardebili MA, Mirzabozorg H (2013) Feasibility study of Dez arch dam heightening based on nonlinear numerical analysis of existing damArchives of Civil Engineering, 59(1):21-49, https://doi.org/ 10.2478/ace-2013-0002
22. Hariri-Ardebili MA, Saouma VE, Porter KA (2016) Quantification of seismic potential failure modes in concrete damsEarthquake Engineering & Structural Dynamics, 45(6):979-997, https://doi.org/ 10.1002/eqe.2697
23. Pouraminian M, Ghaemian M (2015) Shape optimization of concrete open spandrel arch bridges, GRADEVINAR, 67(12):1177-1185, https://doi.org/10.14256/JCE.1223.2015
24. Pourbakhshian S, Ghaemian M (2015) Investigating stage construction in high concrete arch damsIndian Journal of Science and Technology, 8(14):1-4, https://doi.org/10.17485/ijst/2015/v8i14/69510
25. Kim IY, De Weck, OL (2005) Adaptive weighted-sum method for bi-objective optimization: Pareto front generationStructural and multidisciplinary optimization, 29(2):149-158, https://doi.org/10.1007/s00158-004-0465-1
26. Spall JC (1998) An overview of the simultaneous perturbation method for efficient optimizationJohns Hopkins apl technical digest, 19(4):482-492.
27. Pouraminian M, Pourbakhshian S, & Farsangi EN (2020) Reliability assessment and sensitivity analysis of concrete gravity dams by considering uncertainty in reservoir water levels and dam body materialsCivil and Environmental Engineering Reports, 30(1), 1-17, https://doi.org/10.2478/ceer-2020-0001
28. Raphael JM (1984) Tensile strength of concrete, in ACI Journal Proceedings, 158-165.
29. Seyedpoor SM., Salajegheh J, Salajegheh E, & Gholizadeh S (2011) Optimal design of arch dams subjected to earthquake loading by a combination of simultaneous perturbation stochastic approximation and particle swarm algorithmsApplied Soft Computing, 11(1), 39-48 https://doi.org/10.1016/j.asoc.2009.10.014

© 2020 by the authors. Licensee SCU, Ahvaz, Iran. This article is an open access article distributed under the terms and conditions of the Creative Commons Attribution 4.0 International (CC BY 4.0 license) (http://creativecommons.org/licenses/by/4.0/).